

Available online at [www.sciencedirect.com](http://www.sciencedirect.com)

SciVerse ScienceDirect

Nuclear Physics A 904–905 (2013) 755c–758c

[www.elsevier.com/locate/nuclphysa](http://www.elsevier.com/locate/nuclphysa)

# Neutral meson production in $pp$ and $Pb - Pb$ collisions at the LHC measured with ALICE

D.Peresunko (for the ALICE Collaboration)<sup>1</sup>*RRC "Kurchatov institute, Kurchatov sq.,1, Moscow*

---

## Abstract

We present spectra of  $\pi^0$ ,  $\eta$  and  $\omega$  mesons in  $pp$  collisions and  $\pi^0$  mesons in  $Pb$ - $Pb$  collisions measured with ALICE at LHC energies. The  $\pi^0$  and  $\eta$  mesons are reconstructed via their two-photon decays by two complementary methods, using the electromagnetic calorimeters and photon conversion technique; both measurements show perfect agreement. We measure the nuclear modification factor ( $R_{AA}$ ) of  $\pi^0$  production in  $Pb$ - $Pb$  collisions at different collision centralities and compare with lower energy results and theoretical predictions.

---

## 1. Introduction

Neutral mesons, in particular  $\pi^0$  and  $\eta$  mesons can be reconstructed and clearly identified using two-photon decays in a very wide  $p_T$  range. This makes them an excellent tool both for testing QCD predictions of meson yields in  $pp$  collisions and estimating parton energy loss in  $Pb$ - $Pb$  collisions. With these measurements at LHC energies one can access the Parton Distribution Functions (PDF) and Fragmentation Functions (FF) in new kinematic regions and provide further constraints on their low- $x$  (low- $z$ ) parts. Meson production at LHC energies is dominated by gluon fragmentation up to transverse momentum  $p_T \sim 100$  GeV/ $c$  [1], a kinematic regime which makes them ideal to constrain quark as well as the lesser known gluon FF. Measurement of the nuclear modification factor ( $R_{AA}$ ) of  $\pi^0$  production in  $Pb$ - $Pb$  collisions provides a clear pattern for identified particles and is free from ambiguity, such as that found in the separation of protons, kaons and pions in charged hadron suppression.

## 2. ALICE setup

Photons from neutral meson decays can be detected either in the electromagnetic calorimeters PHOS or EMCAL, or can convert on the material of the inner detectors and be reconstructed via  $e^+e^-$  pair in the central tracking system. All three identification methods can be used to provide three independent measurements simultaneously. Below results obtained with PHOS and photon conversion method are presented.

The electromagnetic calorimeter PHOS [3] is made of  $PbWO_4$  crystals and has fine granularity (crystal size  $2.2 \times 2.2 \times 18$  cm<sup>3</sup> installed at the distance 4.6 m from the interaction point),

---

<sup>1</sup>A list of members of the ALICE Collaboration and acknowledgements can be found at the end of this issue.

© CERN for the benefit of the ALICE Collaboration.

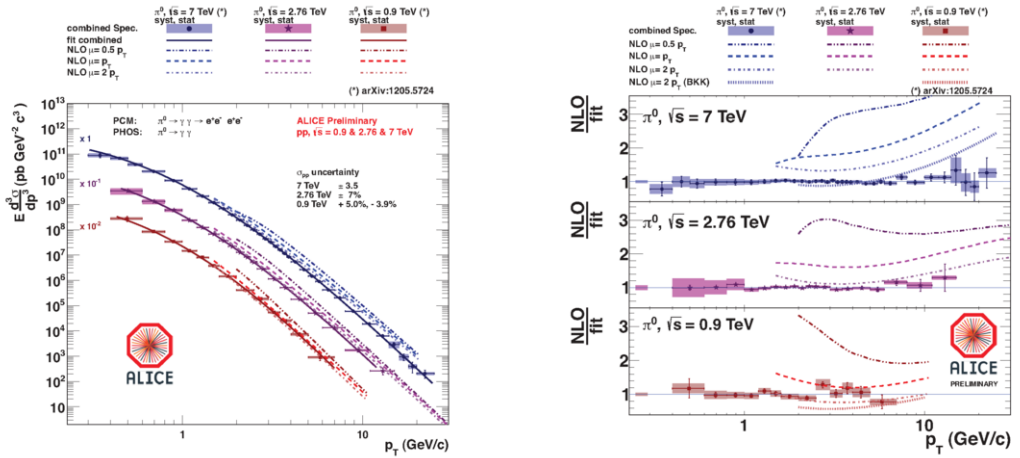


Figure 1: (Color online). Left plot: Spectra of  $\pi^0$  measured in pp collisions at 3 colliding energies, compared to the NLO pQCD predictions and Tsallis fit. Right plot: Ratio data/Tsallis fit compared to the ratio NLO pQCD predictions/Tsallis fit. Theory curves reproduce data at  $\sqrt{s} = 0.9$  TeV but overpredict at 2.76 and 7 TeV [2].

good energy and position resolutions. PHOS covers  $|\eta| < 0.125$  in pseudorapidity and  $60^\circ$  in azimuthal angle with the 3 modules currently installed. Effort was made to reduce the material budget in front of PHOS as much as possible:  $0.2 \cdot X_0$ . Thanks to these conditions PHOS can resolve two photons from  $\pi^0$  decay up to  $p_T^\pi \sim 50$  GeV/c.

In the case of conversion technique, tracks are reconstructed in the ALICE tracking system, consisting of the Inner Tracking System (ITS) [4] and the Time Projection Chamber (TPC). The candidate track pairs are selected using a secondary vertex (V0) finding algorithm. Further refining of the photon sample and rejection of contaminations like  $K_S^0$ ,  $\Lambda$ ,  $\bar{\Lambda}$  is performed using electron identification via  $dE/dx$  and a cut on the opening angle of the pairs.

### 3. pp collisions

ALICE has measured with the 2010 data set  $\pi^0$  spectra at three colliding energies, see fig. 1. Collected statistics corresponds approximately to an integrated luminosity of  $0.14 \text{ nb}^{-1}$ ,  $0.7 \text{ nb}^{-1}$  and  $5.6 \text{ nb}^{-1}$  for energies  $\sqrt{s} = 0.9, 2.76$  and  $7$  TeV, respectively. Spectra were measured independently with PCM and PHOS, results which were in agreement and were subsequently combined into a final spectrum. The measured spectra were compared with NLO pQCD predictions [6]. For the better comparison we fit spectra with the Tsallis parameterization (solid lines in the left plot of fig. 1) and present the data-to-fit ratio with the predictions-to-fit ratio in the right plot. We find that theoretical calculations reproduce  $\pi^0$  spectrum at  $\sqrt{s} = 900$  GeV but considerably overestimate the  $\pi^0$  yield at higher energies.

Using the same data, ALICE measured the spectrum of  $\eta$  meson in pp collisions at  $\sqrt{s} = 7$  TeV [2]. Comparison of the  $\eta$  meson spectrum with theoretical predictions is similar to that of  $\pi^0$ : NLO pQCD predictions overestimate yield. From the measured spectra, the ratio  $\eta/\pi^0$  was constructed. The ratio agrees with measurements at lower energies. In contrast to the spectra, the meson ratio agrees well with NLO predictions.

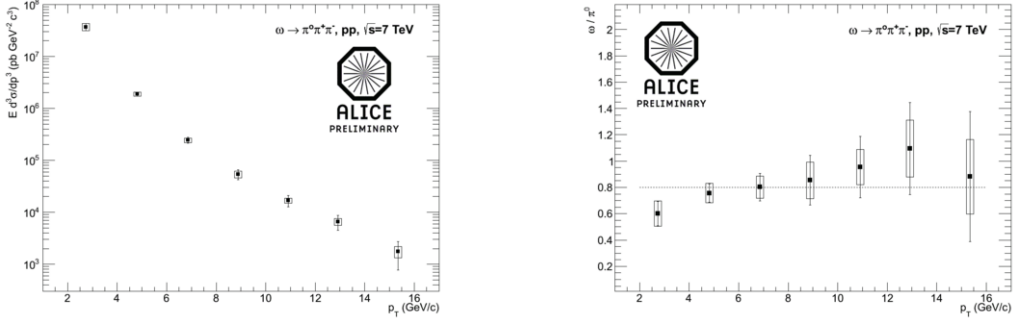


Figure 2: Left: spectrum of  $\omega$  meson measured in pp collisions at  $\sqrt{s} = 7$  TeV. Right: Ratio  $\omega/\pi^0$  measured in pp collisions at  $\sqrt{s} = 7$  TeV. Dashed line – world average of asymptotic ratios measured in pp collisions at lower energies.

In addition to  $\pi^0$  and  $\eta$  meson spectra, the spectrum of  $\omega$  meson was measured in pp collisions at  $\sqrt{s} = 7$  TeV. In the low multiplicity environment of pp collision the best decay channel is  $\omega \rightarrow \pi^0\pi^+\pi^-$  with the branching ratio of 89.2%. We present the results obtained with the 2010 data set. 400 Mevents were analyzed corresponding approximately to an integrated luminosity of  $6 \text{ nb}^{-1}$ . Charged pions were reconstructed in the central tracking system and  $\pi^0$ s were detected in PHOS. The spectrum is shown in fig. 2, left plot. Unfortunately, as the  $\omega$  meson fragmentation function is not yet known currently, there are no NLO predictions available. The measurement of the  $\omega$  spectrum in a wide  $p_T$  range by ALICE can be used as an input for theoretical constrains on parametrization of the  $\omega$  FF. The ratio  $\omega/\pi^0$  is shown in the right plot. We found that slopes of the spectra are close at high  $p_T \gtrsim 4 \text{ GeV}/c$ , and the relative yield of  $\omega$  agrees with world average calculated for pp collisions at lower energies  $\sim 0.8$  [7] shown with dashed line.

#### 4. Pb-Pb collisions

A-A collisions are characterized by a high detector occupancy resulting in considerable probability of cluster overlaps and large combinatorial background. Nevertheless ALICE extracted  $\pi^0$  spectra in several centrality bins in Pb-Pb collisions at  $\sqrt{s_{NN}} = 2.76$  TeV. Using baseline measurements in pp collisions at the same energy, a nuclear modification factor  $R_{AA}$  was constructed. We present  $R_{AA}$  measured in 20% of the most central collisions (fig. 3, left plot). It is compared with  $R_{AA}$  measured at lower energies with WA98 [8] and PHENIX [9] collaborations. We find that starting from the lowest RHIC energy,  $R_{AA}$  has approximately the same shape. Furthermore, the amount of suppression gradually increases with increasing energy of the collision.

We compare the measured nuclear modification factors with several theoretical predictions to be described hereafter (see fig. 3, right plot). The WHDG model [10] takes into account collisional and radiative parton energy loss and geometrical path length fluctuations. The color charge density of the medium is assumed to be proportional to the number of participating nucleons from the Glauber model. The WHDG model reproduces both strength of the suppression and its centrality dependence. Higher twist calculations [11] differ from the WHDG model in the implementation of the medium properties. In addition, the space-time evolution of the medium is described with a  $3 + 1$  dimensional ideal hydrodynamics. Its predictions agree with data in central collisions but fail to reproduce the centrality dependence. Two calculations [12] consider

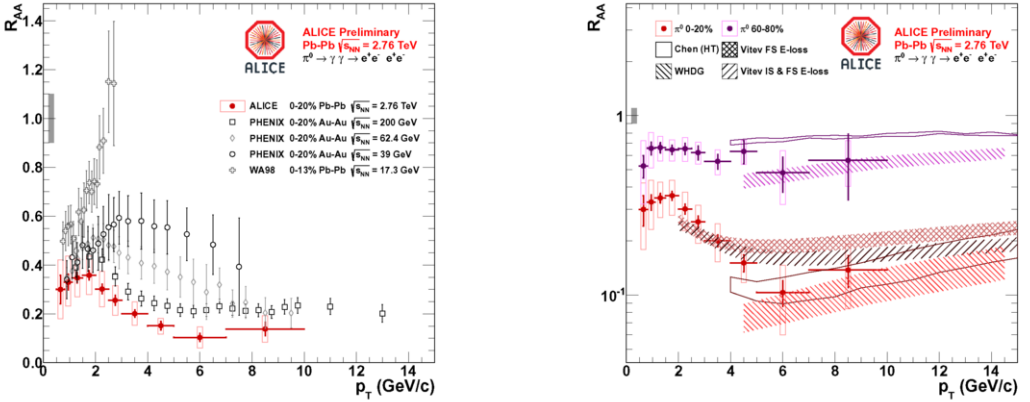


Figure 3: (Color online) Left plot:  $\pi^0$  nuclear modification factor ( $R_{AA}$ ) measured in 20% most central Pb-Pb collisions compared to  $R_{AA}$  in Pb-Pb and Au-Au collisions at lower energies. Right plot:  $R_{AA}$  in 20% of most central and 60-80% peripheral collisions compared to several theoretical predictions.

two cases: incorporate only final-state parton energy loss; take into account energy loss of the incoming parton and the broadening of the transverse momenta of the incoming partons in the cold nuclear matter. Both calculations agree with data, however a somewhat improved agreement is reached if both initial state and final state emissions are taken into account.

## 5. Summary

We presented neutral meson spectra measured by ALICE collaboration in pp collisions at three collision energies and  $R_{AA}$  of  $\pi^0$  measured in Pb-Pb collisions. Spectra measured with two different techniques, with PHOS and with photon conversion method, show good agreement. We found that NLO pQCD predictions describe well  $\pi^0$  and  $\eta$  production in pp at  $\sqrt{s} = 0.9$  TeV, but overestimate their production at  $\sqrt{s} = 2.76$  and 7 TeV. We presented the spectrum of  $\omega$  meson in pp collisions at  $\sqrt{s} = 7$  TeV and found  $\omega/\pi^0$  ratio in agreement with ratios measured at lower energies. Suppression of  $\pi^0$  in Pb-Pb collisions at  $\sqrt{s_{NN}} = 2.76$  TeV is stronger than the one measured at RHIC energies.

This work was partially supported by Russian RFBR grant 12-02-91527.

## References

- [1] R. Sassot et al., Phys. Rev. **D82**, 074011 (2010). P. Chiappetta et al., Nucl. Phys. **B 412**, 3 (1994)
- [2] B. Abelev et al. [ALICE Collaboration], Phys. Lett. **B 717** 162 (2012)
- [3] G. Dellacasa et al., Photon Spectrometer PHOS, Technical Design Report. CERN/LHCC 99-4, 5 March 1999.
- [4] K. Aamodt et al. [ALICE Collaboration], JINST **3**, S08002 (2008)
- [5] J. Alme et al., Nucl. Instrum. Meth. **A622**, 316 (2010)
- [6] P. Aurenche, M. Fontannaz, J. P. Guillet, B. A. Kniehler, M. Werlen, Eur. Phys. J. **C13**, 347 (2000)
- [7] A. Adare et al., Phys. Rev. **C 84**, 044902 (2011)
- [8] M.M. Aggarwal et al., Phys.Rev.Lett. **100**, 242301 (2008)
- [9] A. Adare et al., arxiv:1204.1526. A. Adare et al., Phys.Rev.Lett. **101**, 232301 (2008)
- [10] W.A. Horowitz, Int.J.Mod.Phys. **E16**, 2193 (2007).
- [11] X.-F. Chen et al., Phys.Rev. **C84**, 034902 (2011)
- [12] R. Sharma et al., Phys.Rev. **C80**, 054902 (2009). R.B. Neufeld et al., Phys.Lett. **B704**, 590 (2011)